Supporting Information

Three new AIE-cored Luminescent Cd-based MOF with high quantum yields and selective detection of ions in aqueous media

Wei-Min Chen,[a] Yi Zhang, [a] Zhen-Dong Xue, [a] Hao-Yu Zhu, [a] Qiang Gao, [a] Li-Zhuang Chen [a] and Fang-Ming Wang [*, a]

[a] *School of Environmental and Chemical Engineering, Jiangsu University of Science and Technology, Zhenjiang, Jiangsu 212003, China Email: wangfmzj@qq.com*

Table S1. Selected bond lengths (Å) and bond angles (°) of LMOF-1

Bond	Dist.	Bond	Dist.	Bond	Dist.
Cd-N1	2.292(2)	Cd-O1	2.383(8)	Cd-O3	2.000(6)
Cd-N2	2.381(8)	Cd-O2	2.324(6)	Cd-O4	2.372(4)
Angle	(°)	Angle	(°)	Angle	(°)
N1-Cd-N2	98.4(3)	O1-Cd-O2	55.9(2)	O3-Cd-O4	87.9(3)
N1-Cd-O3	107.2(3)	N2-Cd-O1	84.9(3)	O2-Cd-O4	88.3(3)

Table S2. Selected bond lengths (Å) and bond angles (°) of LMOF-2

Bond	Dist.	Bond	Dist.	Bond	Dist.
Cd1-N1	2.312	Cd1-O1	2.574(9)	Cd1-O3	2.303(7)
Cd1-N2	2.360(3)	Cd1-O2	2.2770	Cd1-O4	2.555(4)
Angle	(°)	Angle	(°)	Angle	(°)
N1-Cd1-N2	84.2(3)	O1-Cd1-O2	52.5(3)	O3-Cd1-O4	53.6(2)
N1-Cd1-O4	87.0(2)	N2-Cd1-O1	89.1(2)	O2-Cd1-O3	83.6(3)

Table S3. Selected bond lengths (Å) and bond angles (°) of LMOF-3

Bond	Dist.	Bond	Dist.	Bond	Dist.
Cd1-N1	2.338(9)	Cd1-O1	2.359(2)	Cd1-O3	2.213(9)
Cd1-N2	2.326(7)	Cd1-O2	2.400(8)	Cd1-O4	2.2320
Cd2-N3	2.338(9)	Cd2-O5	2.400(8)	Cd2-O7	2.2320
Cd2-N4	2.326(7)	Cd2-O6	2.359(2)	Cd2-O8	2.213(9)
Angle	(°)	Angle	(°)	Angle	(°)
N2-Cd1-N1	175.66(14)	O4-Cd1-N1	90.15(71)	O1-Cd1-O2	55.08(11)
O3-Cd1-N1	94.44(71)	O1-Cd1-N2	81.02(81)	O3-Cd1-O4	119.36(91)
O5-Cd2-O7	90.51(41)	N4-Cd2-O8	89.17(41)	N3-Cd2-O6	93.96(01)

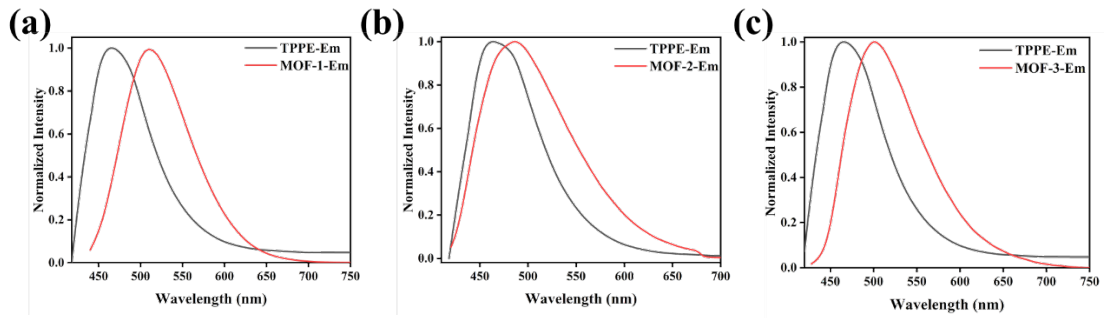

Fig. S1. (a) Emission spectra: (a) **LMOF-1** and TPPE, (b) **LMOF-2** and TPPE, (c) **LMOF-3** and TPPE.

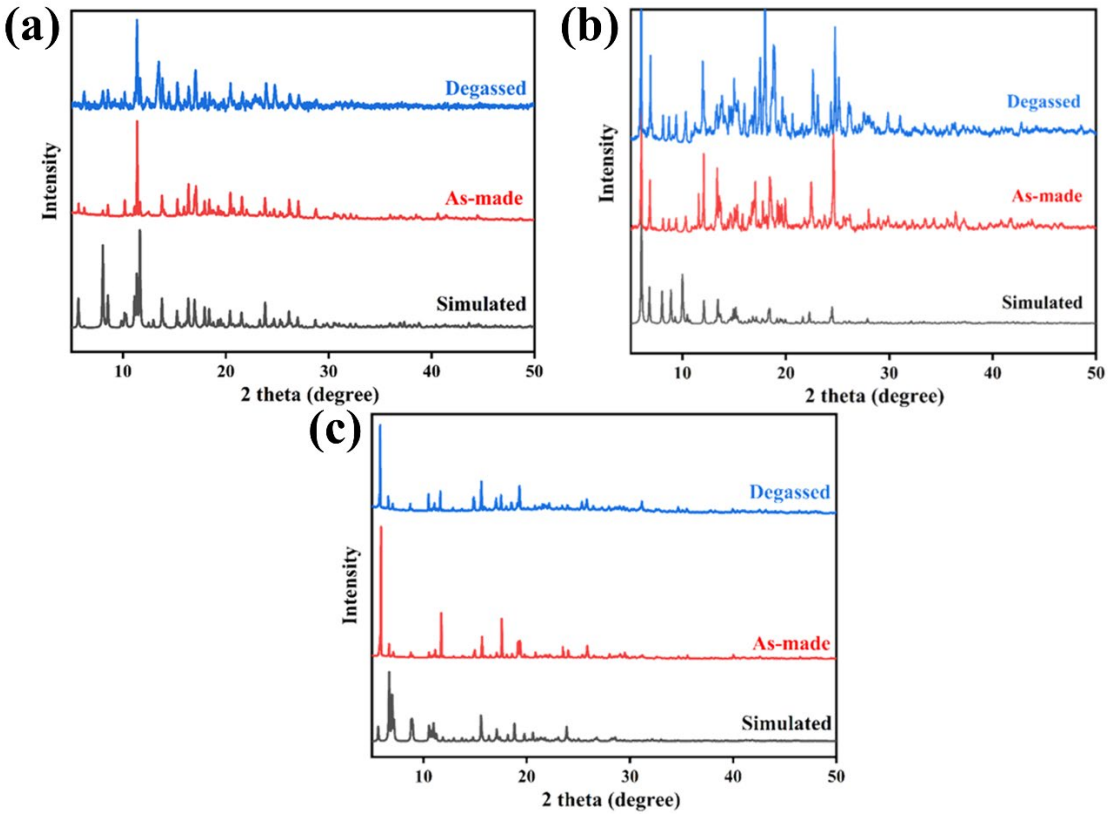

Fig. S2. PXRD pattern of (a) **LMOF-1**, (b) **LMOF-2**, (c) **LMOF-3**.

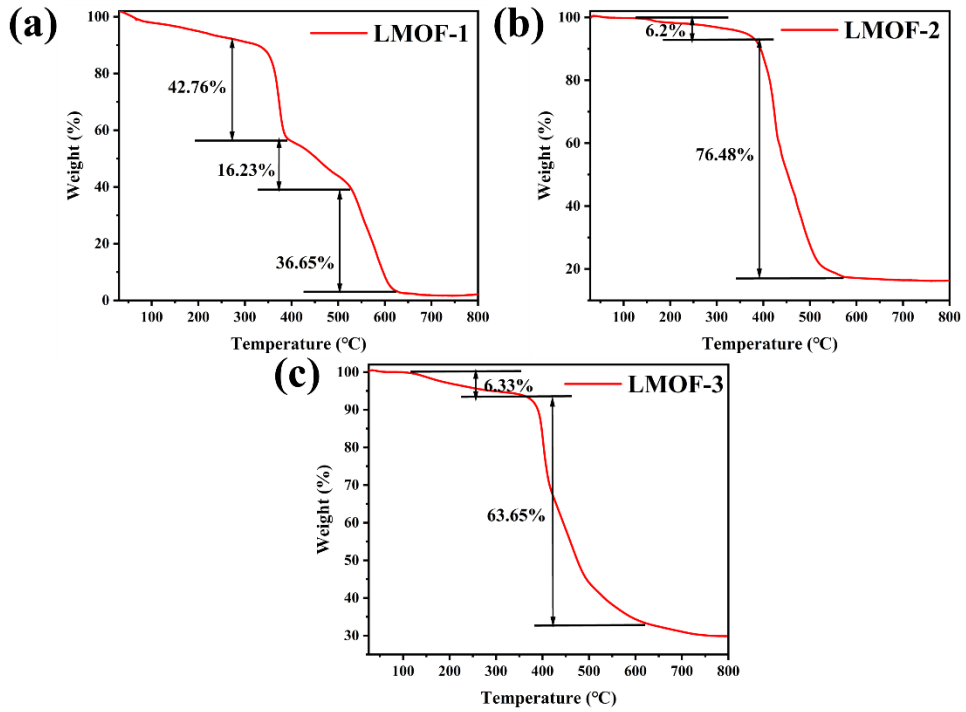

Fig. S3. Thermogravimetric analysis curve of (a) **LMOF-1**, (b) **LMOF-2**, (c) **LMOF-3**.

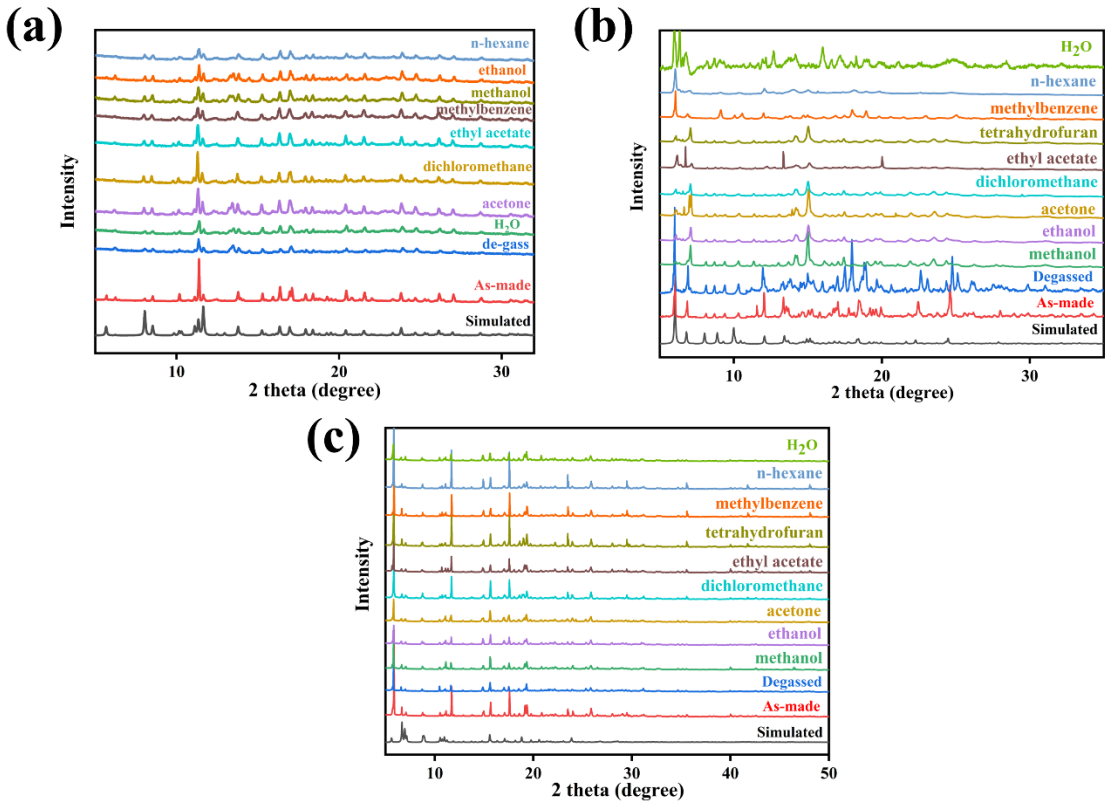

Fig. S4. PXRD patterns of (a) **LMOF-1**, (b) **LMOF-2**, (c) **LMOF-3** after overnight soaking in various solvents.

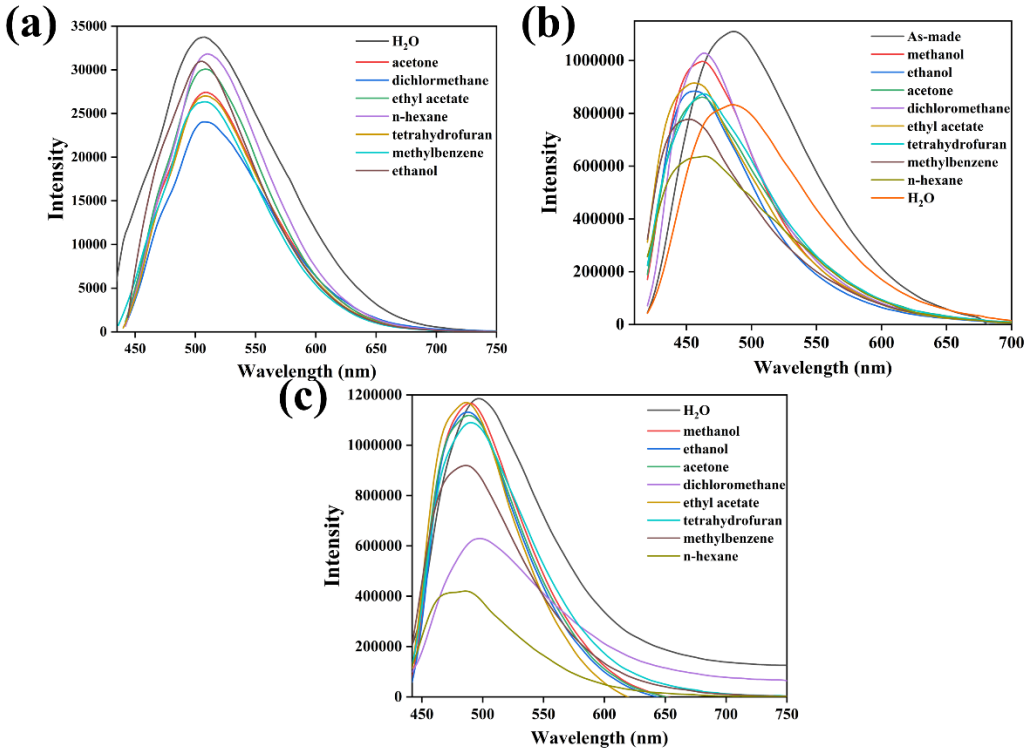

Fig. S5. Emission spectra of (a) **LMOF-1**, (b) **LMOF-2**, (c) **LMOF-3** after soaking in various solvents for 24 hours.

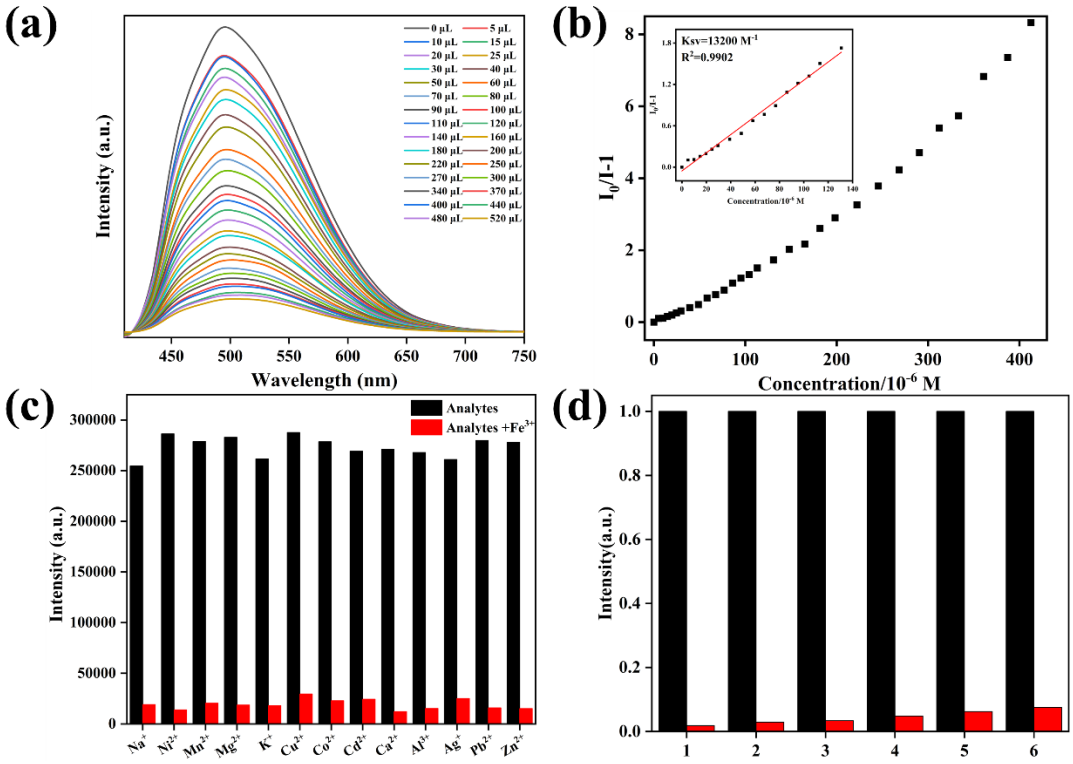

Fig. S6. (a) Intensity change diagram of gradually adding Fe^{3+} solution, (b) S-V fitting curve of Fe^{3+}, (c) Anti-interference experiment with the addition of other ions, (d) Cyclic repetitive experiment in detecting Fe^{3+}in water, of **LMOF-1** suspension.

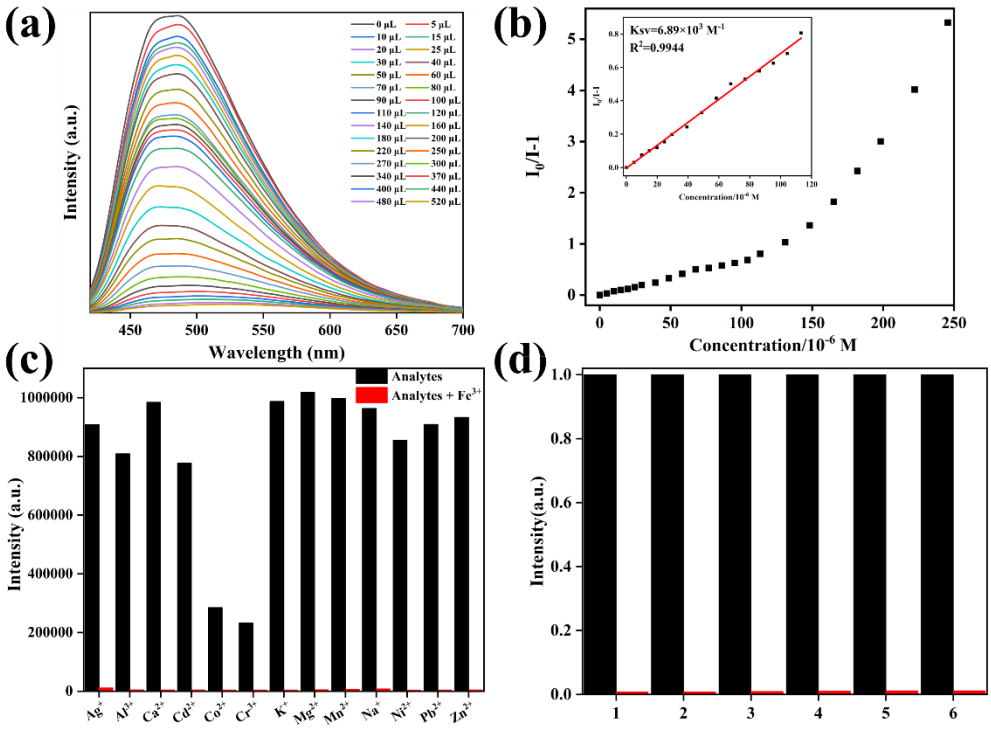

Fig. S7. (a) Intensity change diagram of gradually adding Fe^{3+} solution, (b) S-V fitting curve of Fe^{3+}, (c) Anti-interference experiment with the addition of other ions, (d) Cyclic repetitive experiment in detecting Fe^{3+}in water, of **LMOF-2** suspension.

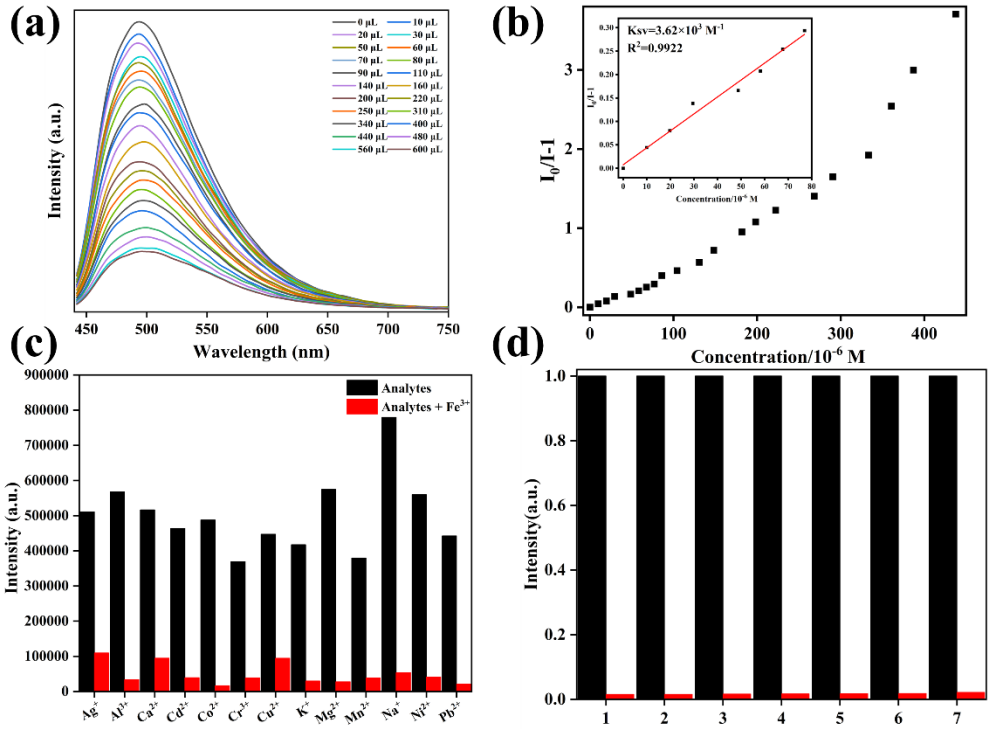

Fig. S8. (a) Intensity change diagram of gradually adding Fe^{3+} solution, (b) S-V fitting curve of Fe^{3+}, (c) Anti-interference experiment with the addition of other ions, (d) Cyclic repetitive experiment in detecting Fe^{3+} in water, of **LMOF-3** suspension.

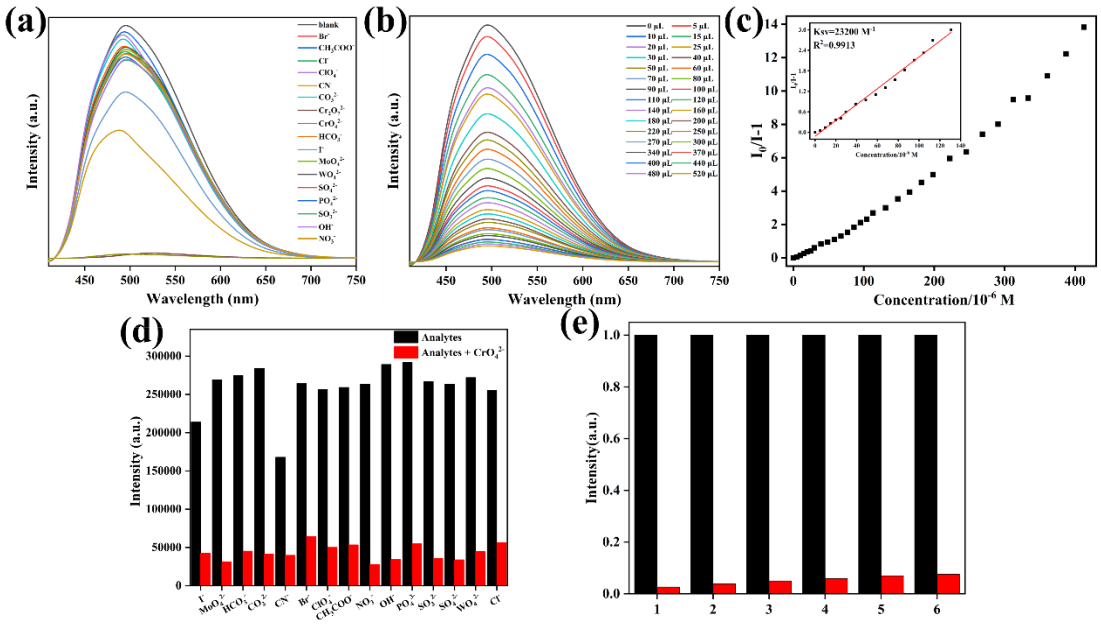

Fig. S9. (a) The luminescence spectra of **LMOF-1** suspension upon adding different anions. (b) The fluorescence intensity trend chart of **LMOF-1** after adding CrO_4^{2-} solution. (c) The SV curves of **LMOF-1** after adding CrO_4^{2-} solution. (d) Anti-interference experiment of selective recognition of CrO_4^{2-}. (e) Reproducibility experiment of **LMOF-1** in detecting CrO_4^{2-} in water

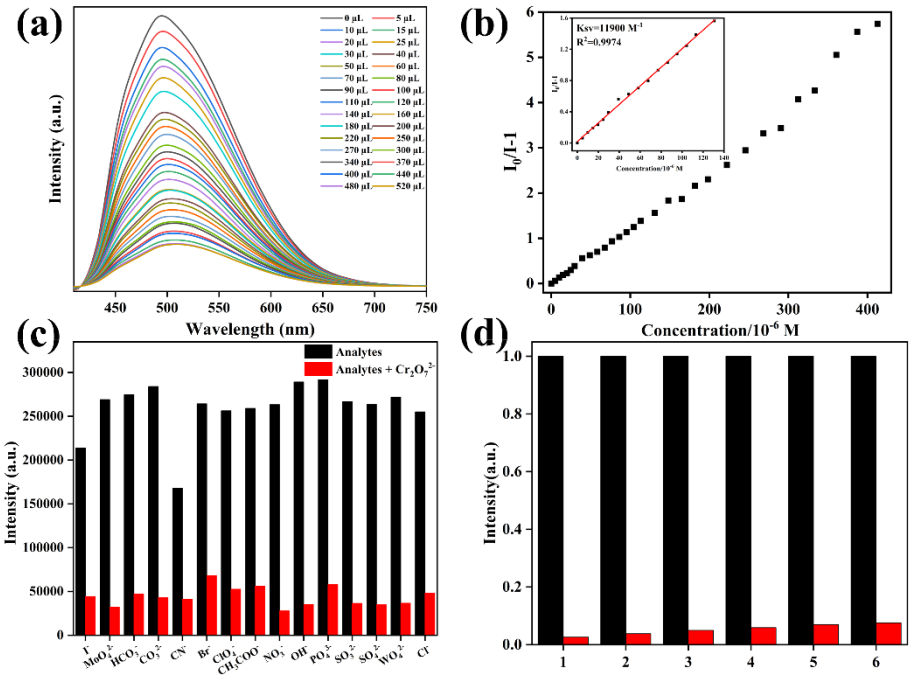

Fig. S10. (a) The fluorescence intensity trend chart of **LMOF-1** after adding $Cr_2O_7^{2-}$ solution. (b) The SV curves of **LMOF-1** after adding $Cr_2O_7^{2-}$ solution. (c) Anti-interference experiment of selective recognition of $Cr_2O_7^{2-}$. (d) Reproducibility experiment of **LMOF-1** in detecting $Cr_2O_7^{2-}$ in water

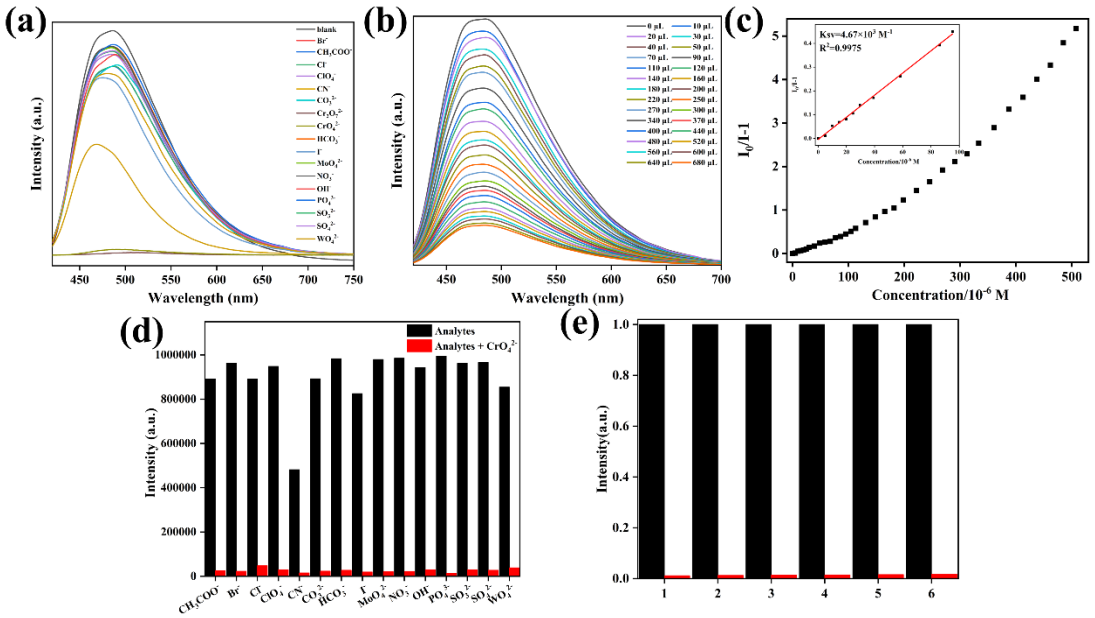

Fig. S11. (a) The luminescence spectra of **LMOF-2** suspension upon adding different anions. (b) The fluorescence intensity trend chart of **LMOF-2** after adding CrO_4^{2-} solution. (c) The SV curves of **LMOF-2** after adding CrO_4^{2-} solution. (d) Anti-interference experiment of selective recognition of CrO_4^{2-}. (e) Reproducibility experiment of **LMOF-2** in detecting CrO_4^{2-} in water

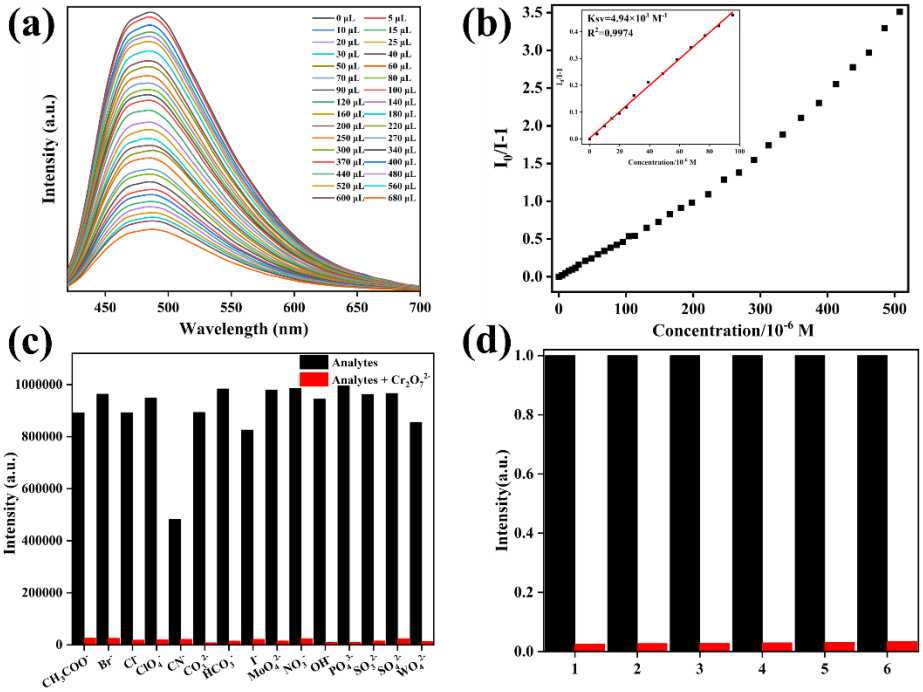

Fig. S12. (a) The fluorescence intensity trend chart of **LMOF-2** after adding $Cr_2O_7^{2-}$ solution. (b) The SV curves of **LMOF-2** after adding $Cr_2O_7^{2-}$ solution. (c) Anti-interference experiment of selective recognition of $Cr_2O_7^{2-}$. (d) Reproducibility experiment of **LMOF-2** in detecting $Cr_2O_7^{2-}$ in water

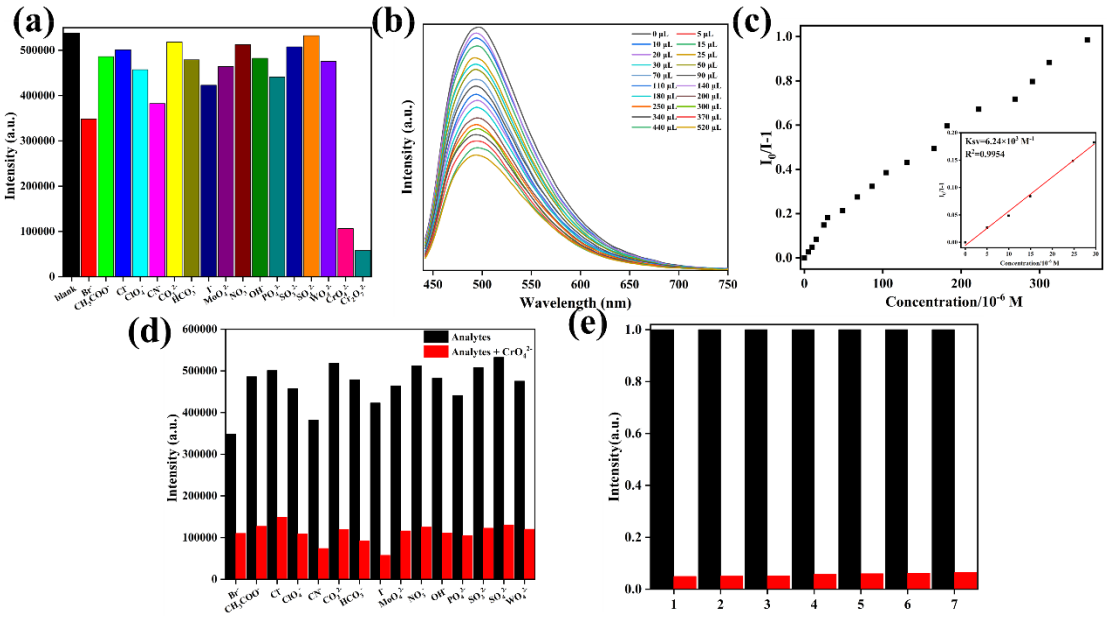

Fig. S13. (a) The luminescence spectra of **LMOF-3** suspension upon adding different anions. (b) The fluorescence intensity trend chart of **LMOF-3** after adding CrO_4^{2-} solution. (c) The SV curves of **LMOF-3** after adding CrO_4^{2-} solution. (d) Anti-interference experiment of selective recognition of CrO_4^{2-}. (e) Reproducibility experiment of **LMOF-3** in detecting CrO_4^{2-} in water

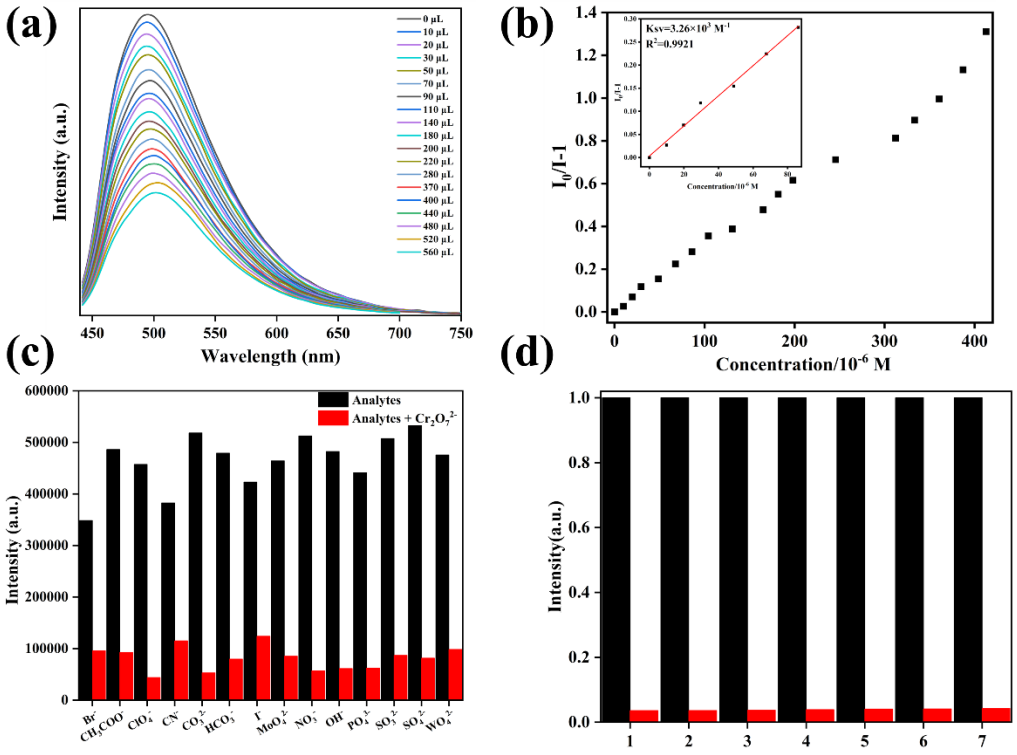

Fig. S14. (a) The fluorescence intensity trend chart of **LMOF-3** after adding $Cr_2O_7^{2-}$ solution. (b) The SV curves of **LMOF-3** after adding $Cr_2O_7^{2-}$ solution. (c) Anti-interference experiment of selective recognition of $Cr_2O_7^{2-}$. (d) Reproducibility experiment of **LMOF-3** in detecting $Cr_2O_7^{2-}$ in water

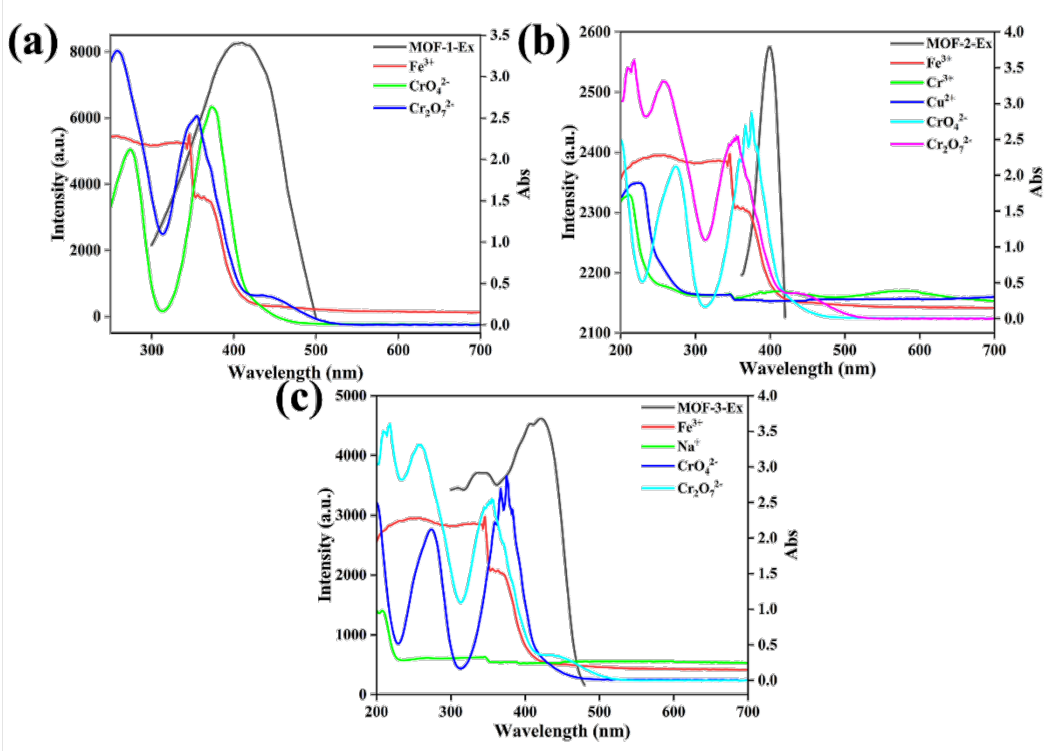

Fig. S15. (a) The UV-vis absorption spectra of Fe^{3+}, CrO_4^{2-} and $Cr_2O_7^{2-}$ and the excitation spectra of **LMOF-1**. (b) The UV-vis absorption spectra of Fe^{3+}, Cr^{3+}, Cu^{2+}, CrO_4^{2-} and $Cr_2O_7^{2-}$ and the excitation spectra of **LMOF-2**. (c) The UV-vis absorption spectra of Fe^{3+}, Na^{+}, CrO_4^{2-} and $Cr_2O_7^{2-}$ and the excitation spectra of **LMOF-3**.

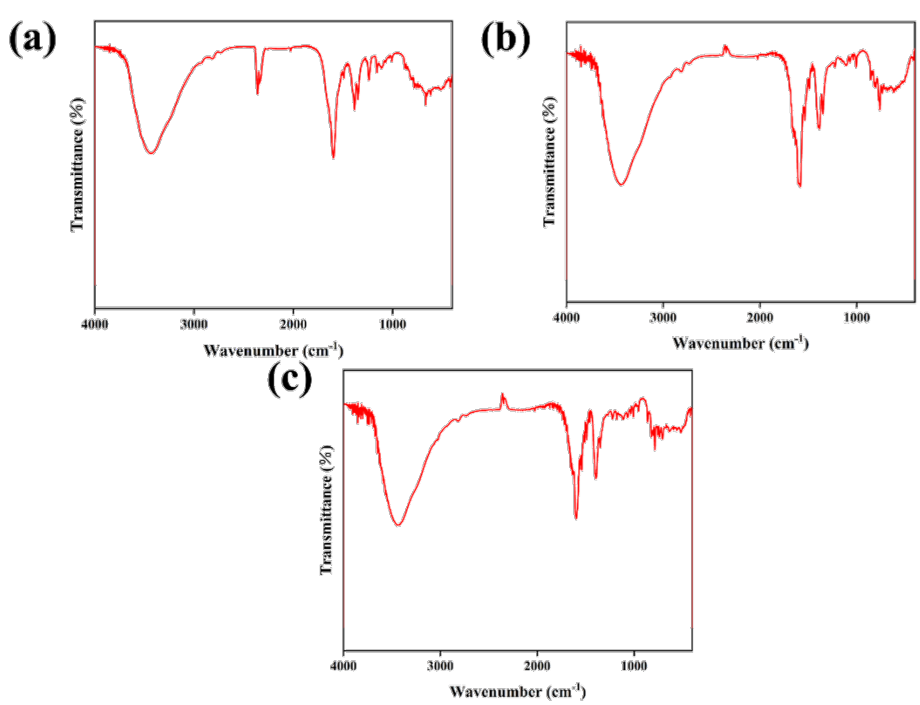

Fig. S16. FT-IR of (a) **LMOF-1**, (b) **LMOF-2**, (c) **LMOF-3**.